Correlation effects in the ground state of Ni-(Co)-Mn-Sn Heusler compounds

Barbiellini Bernardo, Pulkkinen Aki, Nokelainen Johannes, Buchelnikov Vasiliy, Sokolovskiy Vladimir, Miroshkina Olga N., Zagrebin Mikhail, Pussi Katariina, Lähderanta Erkki, Granovsky Alexander

DOI: 10.1557/adv.2019.134

Correlation effects in the ground state of Ni-(Co)-Mn-Sn Heusler compounds

Bernardo Barbiellini[1,2], Aki Pulkkinen[1] , Johannes Nokelainen[1] , Vasiliy Buchelnikov[3,4], Vladimir Sokolovskiy[3,4], Olga N. Miroshkina[3], Mikhail Zagrebin[3,4,5], Katariina Pussi[1], Erkki Lähderanta[1] and Alexander Granovsky[6]

1. Department of Physics, LUT University, FI-53851 Lappeenranta, Finland

2. Department of Physics, Northeastern University, Boston, MA 02445, U.S.A.

3. Faculty of Physics, Chelyabinsk State University, 454001 Chelyabinsk, Russia

4. National University of Science and Technology "MISiS", 119049 Moscow, Russia

5. National Research South Ural State University, 454080 Chelyabinsk, Russia

6. Department of Physics, Lomonosov Moscow State University, 119991 Moscow, Russia

Abstract

We present density functional theory calculations to study the interplay between magnetic and structural properties in Ni-Co-Mn-Sn. The relative stability of austenite (cubic) and martensite (tetragonal) phases depends critically on the magnetic interactions between Mn atoms. While the standard generalized gradient approximation (GGA) stabilizes the latter phase, correlation effects beyond GGA tend to suppress this effect. Mn atoms treated as magnetic impurities can explain our results, where a delicate balance between magnetic interactions mediated by Ni d and Sn p orbitals determines the equilibrium structure of the crystal. Finally, we discuss the role of Co doping in stabilizing ferromagnetic austenite phases.

INTRODUCTION

Ni-Co-Mn-Sn based Heusler alloys display remarkable magneto-caloric effects [1-3], which are consequence of the strong coupling between magnetism and structure arising from the martensitic transition as the sample is cooled. Stoichiometric Heusler alloys have a generic formula X_2YZ and display cubic structure at high temperature. The magnetism is due to 3d electrons from X and Y transition metals. In Ni-Co-Mn-Sn alloys, the magnetic moments are mostly localized at Mn atoms that are magnetically coupled

through an oscillatory interaction mediated by the conduction electrons. Consequently, the magnetic behavior of these alloys is extremely sensitive to the distance between Mn atoms. In this work, we study structural, magnetic and electronic properties of Ni_4Mn_3Sn and Ni_3CoMn_3Sn in eight atom simulation cells by using the density functional theory (DFT) with different approximations for describing correlation effects beyond the local density approximation. Standard DFT simulations use the generalized gradient approximation (GGA) while the strongly constrained and appropriately normed (SCAN) meta-GGA contains correlation corrections beyond the GGA [4]. In practice, SCAN behaves like a DFT+U approach but it avoids the Hubbard term U as an external parameter. To better understand the effect of on-site repulsion energy captured by SCAN, one can consider Heusler compounds for which GGA fails. In particular, the Heusler compounds Co_2FeSi is a good example since GGA fails to produce a half metallic gap while DFT+U calculations [5] and recent SCAN results [6] reproduce this feature. Since SCAN results agree well the DFT+U, effective Hubbard terms U can be deduced from the SCAN band structure [7]. In this paper we focus on alloys relevant for magneto-caloric effects. A comprehensive study within SCAN for other ternary Heusler alloys have been recently reported by Buchelnikov *et al.* [6].

COMPUTATIONAL METHODS

The VASP code and PAW pseudopotentials were used for the present calculations [8,9]. The plane wave basis kinetic energy cut-off of 550 eV was applied whereas the kinetic energy cut-off for the augmented charge was chosen as 800 eV. The uniform Monkhorst-Pack mesh of 8 x 8 x 8 k-points together with a Gaussian broadening of 0.2 eV were used to integrate the Brillouin zone with the second order Methfessel-Paxton method. To obtain accurate density of states (DOS) curves, non-selfconsistent calculations were performed using 24 x 24 x24 k-points. The simulations were performed in the standard 8-atom supercell of the Heusler alloys with X_2YZ structure (space cubic group No. 225, prototype Cu_2MnAl), which contains four atoms as basis wherein two X atoms occupy 8c (1/4, 1/4, 1/4) and (3/4, 3/4, 3/4), whereas Z and Y atoms are placed at 4a (0, 0, 0) and 4b (1/2, 1/2, 1/2) Wyckoff positions, respectively. For Ni_4Mn_3Sn, a Mn atom replaces a Sn atom of the stoichiometric compound Ni_2MnSn while Ni_3CoMn_3Sn is produced by replacing a Ni atom by a Co atom in Ni_4Mn_3Sn.

RESULTS

Structure optimization calculations are first performed to investigate the ground-state properties for the cubic austenite structure of Ni_4Mn_3Sn without Co using GGA and SCAN. The energy minimum for GGA is at a=5.944 Å while in SCAN the minimum is located at a smaller lattice constant a=5.920 Å. These values are both close to the experimental lattice constant at room temperature a=5.929 Å for the compound $Ni_{40}Co_{10}Mn_{40}Sn_{10}$ [1] with Co. The GGA ground state is ferrimagnetic (FIM) as the Mn spin on the Z position is opposite to the Mn spin on the Y position while the SCAN ground state is ferromagnetic (FM). Figure 1 shows the total energy curves as a function of the tetragonal c/a ratio ranging from 0.80 to 1.50. The volume of the supercell is kept constant while the tetragonal distortion is performed in the total energy calculations. As shown in Fig.1, GGA provides a FIM solution more stable than FM while SCAN reverts this order by stabilizing the FM solution. Both GGA and SCAN achieve the minimum of the energy for an elongated tetragonal cell (c/a>1) but the SCAN solution is more cubic. From DOS result shown in Fig.2(a), one can see that the states around the Fermi level (and thus

responsible for the metallic character of the material) are mostly Ni d states, while Mn d states are largely responsible for the magnetization. In fact, SCAN magnetic moments on Mn, Ni and Sn atoms are about 3.8 μ_B, 0.6 μ_B and 0.0 μ_B respectively while the corresponding PBE values are 3.6 μ_B, 0.57 μ_B and 0.0 μ_B. These results can be rationalized by describing the localized d electrons on Mn atoms as Anderson impurities interacting with a bath of more delocalized Ni d and Sn p electrons [10]. In fact, the Anderson model results in a Rudermann-Kittel-Kasuya-Yosida (RKKY) effective interactions between Mn magnetic moments that is inversely proportional to an effective Hubbard U. Thus, the parameter U suppresses RKKY magnetic interactions and reduces the energetic advantage associated with the deformation of the cubic austenite phase into a tetragonal martensite phase. Figure 2(b) illustrates the effect of the U parameter on the total DOS in GGA+U. Taking into account U makes the DOS more similar to the SCAN one. Moreover the partial magnetic moments approach SCAN corresponding values. The effective Hubbard U of SCAN can give exaggerated magnetic moments for itinerant FM metals such as iron [11-13]. In DFT+U, the same issue can be cured by introducing an exchange parameter J, which is of the order of the Stoner parameter [14,15]. The difference U−J yields a reduced Hubbard effective and a similar correction can be applied to SCAN. However, here, since the d electrons are localized on Mn atoms, the problem encountered in itinerant ferromagnetic systems does not occur. When the Co doping is considered, both the GGA and SCAN yield the cubic FM stable state with large magnetic moment needed for the giant magnetocaloric effect [1,2]. The cubic equilibrium lattice constants remain similar to those calculated without Co: a=5.955 Å for PBE a=5.914 Å for SCAN. Figure 3 shows that upon tetragonal distortion, the FIM distorted solution becomes practically degenerate with the FM solution in GGA but this is not the case in SCAN. Nevertheless, a SCAN ground state with a lower total magnetic moment could appear in a larger simulation cell, where more complicated solutions can be accommodated as in the case of $YBa_2Cu_3O_7$ [16]. Clearly, the existence of low temperature states with low magnetization is vital for the giant magnetocaloric effect. Moreover, the tuning of this effect can be achieved by doping with Co and Al [3] and probably also by forming vacancies and other defects in the Ni-Co-Mn-Sn-Al alloy.

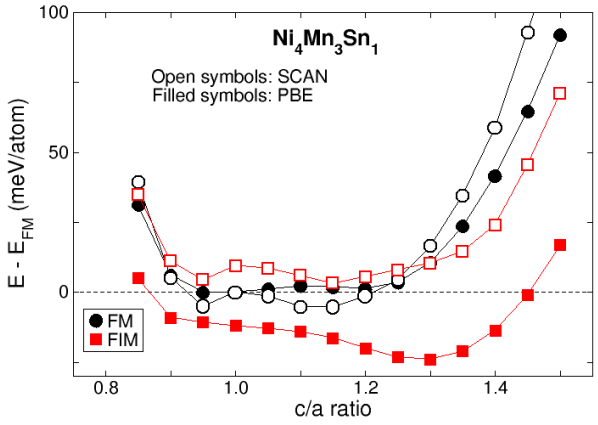

Figure 1. The calculated total energy differences relative to the FM state as a function of the c/a ratio for Ni_4Mn_3Sn.

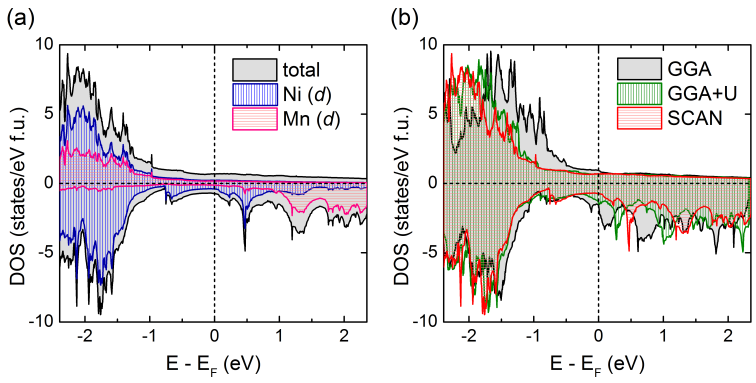

Figure 2. (a) Total and partial DOS calculated with SCAN and (b) total DOS calculated with GGA, GGA +U (U=2 eV and J=0.7 eV) and SCAN for Ni_3Mn_3Sn.

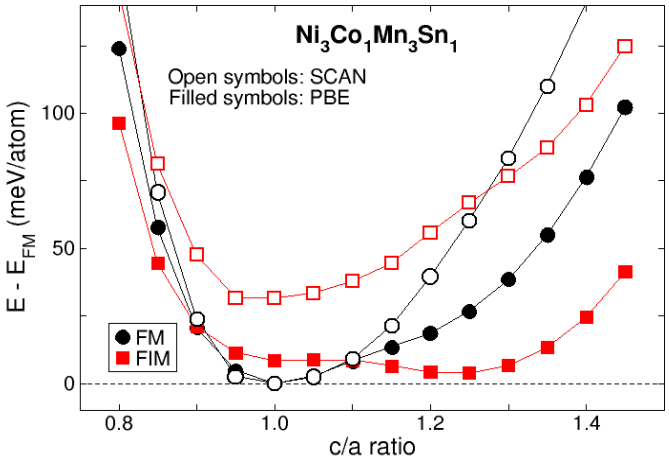

Figure 3. The calculated total energy differences relative to the FM state as a function of the c/a ratio for Ni_3CoMn_3Sn.

CONCLUSION

The present study shows that an accurate account of correlation effects in Ni-Co-Mn-Sn alloys is important in order to predict the relative stabilities of different phases. The simple RKKY interaction between Mn atoms can explain most of the physics of the present systems. Surprisingly, in spite of the metallic character of the Ni-Co-Mn-Sn alloys, correlation effects beyond GGA can significantly modify the description of electron localization and of magnetic properties that play a key role in the giant magnetocaloric effect. Large supercells may be needed in order to accommodate complicated solutions promoted by correlation effects.

ACKNOWLEDGMENTS

This work was supported by RSF-Russian Science Foundation No. 17-72-20022. B.B. acknowledges support from the COST Action CA16218.

REFERENCES

1. L. Huang, D. Y. Cong, H. L. Suo, Y.D. Wang, Appl. Phys. Lett. **104**,132407 (2014).
2. Tino Gottschall, Adria Gracia-Condal, Maximilian Fries, Andreas Taubel, Lukas Pfeuffer, Lluis Manosa, Antoni Planes, Konstantin P. Skokov and Oliver Gutfleisch, Nat. Mat. **17,** 929 (2018).
3. V. Sokolovskiy, M. Zagrebin, V.D. Buchelnikov, J. Magn. Mag. Mater. **459**, 295 (2018).
4. J. Sun, A. Ruzsinszky, J. P. Perdew, Phys. Rev. Lett. **115**, 036402 (2015).
5. B. Balke, G. H. Fecher, H. C. Kandpal, C. Felser, K. Kobayashi, E. Ikenaga, J. J. Kim, and S. Ueda, Phys. Rev. B **74**, 104405 (2006).
6. V. D. Buchelnikov, V. V. Sokolovskiy, O. N. Miroshkina, M. A. Zagrebin, J. Nokelainen, A. Pulkkinen, B. Barbiellini, and E. Lähderanta, Phys. Rev. B **99**, 014426 (2019).
7. C. Lane, J. W. Furness, I. G. Buda, Y. Zhang, R. S. Markiewicz, B. Barbiellini, J. Sun, and A. Bansil, Phys. Rev. B **98**, 125140 (2018).
8. G. Kresse, J. Furthmuller, Phys. Rev. B **54**, 11169 (1996).
9. G. Kresse, D. Joubert, Phys. Rev. B, **59**, 1758 (1999).
10. B. Himmetoglu, V. M. Katukuri, M. Cococcioni, J. Phys.: Cond. Matter **24**, 185501 (2012).
11. E. B. Isaacs, C. Wolverton, Phys. Rev. Mat. **2**, 063801 (2018).
12. M. Ekholm, D. Gambino, H. J. M. Jonson, F. Tasnadi, B. Alling, I. A. Abrikosov, Phys. Rev. B **98**, 094413 (2018).
13. F. Yu, D. J. Singh, Phys. Rev. Lett. **121**, 207201 (2018).
14. M. Cococcioni, PhD Thesis, SISSA (2002).
15. A.G. Petukhov, I.I. Mazin, L. Chioncel, A.I. Lichtenstein, Phys. Rev. B **67**, 153106 (2003).
16. Y. Zhang, C. Lane, J. W. Furness, B. Barbiellini, R. S. Markiewicz, A. Bansil, J. Sun, arXiv:1809.08457 (2018).